EFFECT OF AMMONIA-ETHANOL MOLE RATIO ON THE SILICA NANOPARTICLES SYNTHESIZED FOR RHODAMINE B DYES ADSORPTION

Yayuk Puji Lestari, Amaria Amaria*
Department of Chemistry, Faculty of Mathematics and Natural Science, Universitas Negeri Surabaya, Jl. Ketintang Surabaya 60231, East Java, Indonesia
*Email: amaria@unesa.ac.id

Received 27 March 2023
Accepted 18 May 2023

Abstract

Various ammonia-ethanol mole ratios were successfully used for the synthesis of silica nanoparticles for rhodamine B adsorption. This study aims to determine the characteristics of the adsorbent at different ammonia-ethanol mole ratios, maximum adsorption at pH, and contact time. Several steps, including extraction of Na_2SiO_3 from rice husk ash, synthesis of adsorbents with ammonia-ethanol mole ratios (14:1, 21:1, 28:1, and 42:1), and their characterization. The parameters studied in the adsorbent include the functional groups, particle size, maximum pH, and rate constant adsorption. The FTIR results showed that all adsorbents had functional groups, indicating the presence of silica. The results suggest that the optimum mole ratio of NS 14:1 particles has a size of 39.82 nm. The optimum adsorption of rhodamine B by NS 14:1 occurred at a pH 3 of 0.00419 $mmol.g^{-1}$ and a contact time of 40 min. The rate constant of adsorption by NS 14:1 was 102.42 $g.mmol^{-1}.min^{-1}$ followed a pseudo-second order kinetic model.

Keywords*: adsorption, rhodamine B, silica nanoparticles*

Introduction

Rhodamine B is commonly used in the textile, paper, and batik industries (Kurniasih et al., 2014; Ulya et al., 2022). The use of synthetic dyes, such as rhodamine B, is more desirable than natural dyes because they are cheap, easy to obtain, have strong coloring power, and are easy to use. Rhodamine B contains a primary amino group with a stable benzene core, making it difficult to degrade because it is complex and robust against light (Sahara et al., 2018). According to the Ministry of Environment Decree in Indonesia No. 51 of 1995, the threshold for the concentration of dyes in wastewater is 5 mg/L. The presence of 1 mg/L dye waste causes the water to appear colored, while the color content of textile waste typically ranges from 20 to 200 mg/L. Excessive entry of rhodamine B into the environment is highly toxic to water and disrupts sea microorganisms. In the human body, it can cause serious effects such as poisoning, digestive tract irritation, respiratory tract irritation, skin irritation, and liver cancer (Shofiyani et al., 2020). Therefore, a method to treat waste contaminated with these dyes is required.

Several methods for reducing dyes include adsorption, electrolysis, precipitation, ion exchange, chemical oxidation, and other biological techniques (Kurniasih et al., 2014; Raditya et al., 2016). The adsorption method is widely used because it is more effective and economical, its operation is flexible, simple, and can be recycled. Madina et al. (2017) reported that silica from Bengkulu Long Beach sand occurred maximum adsorption of rhodamine B at an optimum pH of 2 and an optimum contact time of 20 minutes. Zhai (2020) reported that mesoporous nano silica exhibited the maximum adsorption of rhodamine B at

an optimum pH of 5, with contact time of 20 minutes and an 1.30 mg/g adsorption capacity. Adsorption parameters affect the adsorbent capacity for adsorbate adsorption (Asnawati et al., 2017).

The sol-gel process has several advantages, such as the fact that the process takes place at low temperatures, it is relatively easy, the result is highly pure, and the reaction kinetics can be managed by changing the composition of the reaction mixture (Bhatt et al., 2021). The concentrations of the precursors, catalysts, solvents, and gel maturation are critical for synthesizing silica particles on the nano scale. Sodium silicate as a precursor has the advantage that the particle size is finer and more uniform than that of commercial precursors, such as tetraethyl orthosilicate and tetramethyl orthosilicate, which are equally expensive, toxic, and cause environmental problems (Al-Abboodi et al., 2020).

The utilization of various agricultural wastes has been carried out extensively, one of which is rice husk ash, which is abundant and easy to obtain and can be used as an adsorbent because of its relatively high silica content. Previous research conducted by Zulfiqar et al. (2016) synthesis using technical sodium silicate by varying the volume ratio of ammonia and ethanol. The novelty of this research is that the synthesis was carried out using sodium silicate precursors from rice husk ash by varying the ammonia-ethanol mole ratio. The purpose of this study was to determine the characteristics of the adsorbent, optimum pH, and adsorption rate constant. This research is expected to be used as a scientific contribution to efforts to treat waste to reduce environmental pollution due to hazardous waste.

Research Methods

Materials

Rice husk from Lamongan district was used as the research material, hydrochloric acid (Merck), Na_2EDTA, sodium hydroxide (Merck), ammonium hydroxide, ethanol 96%, rhodamine B (Merck), and demineralized water were obtained from Bratachem.

Instrumentation

The research instruments used were an FT-IR spectrophotometer (Thermo Scientific Nicolet iS10), a colorimeter silicate (Merck), a Zetasizer nano ZS (Malvern), and a UV-Vis spectrophotometer (Shimadzu 1800).

Procedure

1) Preparation of ash

   The rice husks were washed with hot water to eliminate contaminants. It was then dried in the sun for 48 hours. The dried rice husks were crushed using a milling machine. Rice husks were ashed in a furnace for 4 hours at 700ºC. The ash was sieved through a 200-mesh sieve (Amaria, 2012).

2) Extraction of Na_2SiO_3

   Five grams of ash were placed in a beaker, and each was added to 50 mL of demineralized water, acidified with 6 M hydrochloric acid up to pH=1, and stirred for 2 h. After acidification, the mixture was rinsed to a neutral pH. The obtained residue was mixed with 20 mL of Na_2EDTA 0,1M. The mixture was stirred again for 1 h using a magnetic stirrer before being filtered and washed with demineralized water. The ash was added to 30 mL of 3.5 M sodium hydroxide and heated with reflux for 1 h. The extracted Na_2SiO_3 solution was filtered using Whatman 42. The volume was then measured and stored in a clean bottle (Amaria, 2012).

3) Synthesis of silica nanoparticles

   The adsorbents were prepared following the procedure of Zulfiqar et al. (2016) with modifications. First, in a polyethylene glass, 5 mL of Na_2SiO_3 was added to 10 mL of demineralized water then stirred for 15 minutes.

Second, 10 mL ethanol was added to the dilute sodium silicate solution and stirred for 30 min. Third, 30 mL of ammonium hydroxide was added and stirred for 30 min, with a mole ratio of ammonia to ethanol of 14:1. The adsorbents were synthesized using the ammonia-ethanol mole ratio, abbreviated as NS (14:1, 21:1, 28:1, and 42:1). After the aging process, the gel was washed with demineralized water up to a neutral pH. The adsorbents were dried at 80ºC in an oven until it reached a constant weight. The obtained silica nanoparticles were sieved using a 100 mesh. Each experiment was characterized using an FTIR spectrophotometer. An analogy of this work by varying the mole ratio of ammonia to ethanol is presented in Table 1.

Table 1. The mole ratio of ammonia to ethanol in the synthesis of silica nanoparticles

Sample	Mole ratio A:E	Si (mmol)	Ammonia (mmol)	Ethanol (mmol)
NS 14:1	14:1	0.355	3.3	46.4
NS 21:1	21:1	0.355	2.2	46.4
NS 28:1	28:1	0.355	1.65	46.4
NS 42:1	42:1	0.355	1.1	46.4

4) Characterization of the adsorbent functional groups

The functional groups of the silica nanoparticles were characterized using an infrared spectrophotometer (FTIR). According to Indrasti et al. (2020), as much as 0.02 grams of silica nanoparticle powder was dispersed in demineralized water and stirred for 15 min. The dispersion was sonicated for 30 minutes, using PSA the samples were examined for 2-5 min.

5) Stability test of silica nanoparticles

The adsorbent (100 mg) was added to a 10 mL solution of pH 4, 5, 6, 7, 8, 9, and 10 and shaken at 400 rpm for 1 h. The mixture was kept for 24 h and then centrifuged at 2000 rpm for 10 min. The remaining silica nanoparticles were separated using filter paper, filtered, and dried at 80 °C until a constant weight was obtained, after which the weight was analyzed (Indrawati and Cahyaningrum, 2013).

6) The pH effect on Rhodamine B adsorption

The NS 14:1 and NS 42:1 adsorbents (50 mg) were mixed with 10 mL of 25 mg/L rhodamine B solution. The pH was adjusted to 2, 3, 4, 5, 6, and 7. The samples were shaken at 250 rpm for 120 min and centrifuged at 2000 rpm for 10 min. The absorbance of the filtrate was measured at a maximum wavelength of 553.5 nm.

7) The contact time effect on Rhodamine B adsorption

The NS 14:1 and NS 42:1 adsorbents (50 mg) were mixed with 10 mL of 25 mg/L rhodamine B solution at the optimum pH. The contact time was varied at 20, 40, 60, 90, 120, 150, 180, and 210 min. The samples were shaken at 250 rpm for different contact times. The absorbance of the filtrate was measured at a maximum wavelength of 553.5 nm.

Results and Discussion

Preparation of ash

The process of producing ash begins by washing the rice husks in hot water to remove any remaining contaminants such as sand or soil. After washing, the rice husks were dried in the sun for 48 hours. The dry rice husks were mashed before

being placed into the furnace to increase their surface area and equalize their size. The refined husks spend time four hours in a furnace at 700ºC. According to Yusmaniar et al. (2017), the decomposition reaction that occurs in the ashing process can be represented by Eq. (1).

$$Element\ C, H\ and\ Si + O_2 \rightarrow SiO_{2(s)} + CO_{2(g)} + H_2O_{(g)} \quad (1)$$

The temperature and time of rice husk ashing can be used to determine the silica crystal structure. Rice husk ashing was carried out at 700 °C for 4 h because this is the optimum temperature for producing ash with an amorphous silica structure (Nopianingsih et al., 2015). If the temperature is below 700ºC, there is still carbon that has not been completely oxidized; therefore, the silica content in the ash is still relatively low. If the temperature is 800ºC and 900ºC, it will produce silica with a crystalline structure is produced. The ashing process of rice husk producing gray-white ash is presented in Figure 1. The ash obtained from several ashing processes was then calculated to determine the rendemen percentage. The results for the rendemen percentage of ash are listed in Table 2.

(**a**) (**b**)

Figure 1. Rice husk, (**a**) before being in the furnace and (**b**) after being in the furnace

Table 2. The percentage of ash rendemen

Weight of rice husk (g)	Weight of rice husk ash (g)	Rendemen
50	8.5	17 %
50	8.1	16.2 %
50	8.6	17.2 %
50	8.5	17 %
50	8.2	16.4 %
50	8.5	17 %
50	8.8	17.6 %
The average rendemen (%)		16.9 %

First, the rice husk ash was reacted with 1 mL of 6 M HCl solution to pH 1 to eliminate contaminants from metal oxides, such as CaO and K_2O (Yusuf et al., 2014). The mixture was stirred for 2 h and washed with demineralized water until neutral pH was achieved. Second, the ash interacted with 20 mL of 0.1 M Na_2EDTA solution to remove impurities still left behind because Na_2EDTA is a metal ion chelating agent (Aini and Amaria, 2022). The ash was rinsed with demineralized water to neutral pH.

Extraction of Na_2SiO_3

The ash was extracted using NaOH solution under reflux (Wulandari and Amaria, 2015). The results of the sodium silicate extraction are presented in Table 3. The resulting sodium silicate was a colorless and viscous solution. The Na_2SiO_3 extraction reaction presented in Eq. (2).

$$SiO_2 + 2\,\mathrm{NaOH} \rightarrow Na_2SiO_3 + H_2O \quad (2)$$

Na_2SiO_3 was measured to determine the Si content using a color comparator at a concentration of 0.01-0.25 mg/L. The results of the analysis of Si concentration using the colorimetric method are presented in Figure 2. The Si concentration of the extracted sodium silicate was 0.071 mmol/mL.

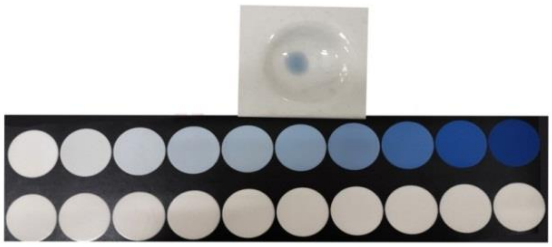

Figure 2. The color comparator of Si concentration using the colorimeter

Table 3. Extraction results of sodium silicate

Mass of Rice Husk Ash (g)	Volume of NaOH (mL)	Volume of Na_2SiO_3 (mL)	Si Concentration (mmol/mL)
5.0009	30	25	0.071
5.0013	30	25	0.071
5.0008	30	25	0.071

Synthesis of silica nanoparticles

The adsorbent was synthesized through several stages: hydrolysis, condensation, aging, and drying. In the hydrolysis process, sodium silicate is dissolved in an ethanol solution and hydrolyzed with water under basic conditions to produce a colloidal sol. The sol-gel reaction process in the base state is shown in Figure 3. Referring to Figure 3, the reaction mechanism for the formation of silica nanoparticles is presented in Eq. (3), (4) and (5), respectively.

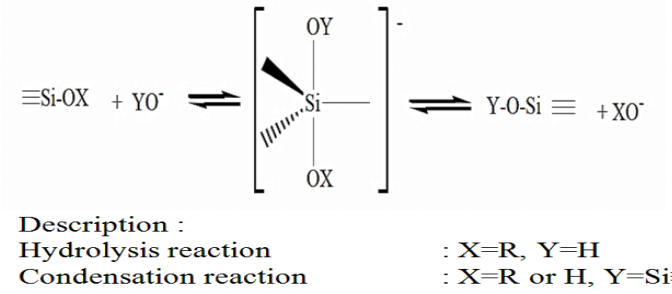

Figure 3. The sol-gel reaction in base conditions (Schubert and Husing, 2000)

Hydrolysis

$$\equiv \mathrm{Si} - \mathrm{OR} + H_2\mathrm{O} + NH_3 \overset{H^+}{\rightarrow} \equiv \mathrm{Si} - \mathrm{OH} + \mathrm{ROH} + \mathrm{N}H_4{}^+ \quad (3)$$

Alcohol condensation

$$\equiv \mathrm{Si} - \mathrm{OH} + RO - Si \equiv \rightarrow \equiv \mathrm{Si} - \mathrm{O} - \mathrm{Si} \equiv + \mathrm{R} - \mathrm{OH} \quad (4)$$

Water condensation

$$\equiv \mathrm{Si} - \mathrm{OH} + HO - Si \equiv \rightarrow \equiv \mathrm{Si} - \mathrm{O} - \mathrm{Si} \equiv + H_2\mathrm{O} \quad (5)$$

Description: R = $-CH_2CH_3$

The ethoxy group (-OR) was replaced with (-OH) during hydrolysis. Beganskiene et al. (2004) reported that the concentrations of the precursor and NH_3 quickly affect hydrolysis. Upon increasing the concentration of the ammonia solution, the H_2O molecules dissociated, resulting in OH^- quickly attacking Si atoms.

The condensation process begins with the hydroxyl group from the hydrolysis reaction process (≡Si-OH) that reacts with ≡Si-OR from another intermediate or with ≡Si-OH from another intermediate to form siloxane (Beganskiene et al., 2004). The rate of condensation in water is faster than that of alcohol condensation (Ibrahim et al., 2010).

After hydrolysis and condensation, the next processes are gelation and aging into a network of gels that are more rigid, strong, and shrink in solution. The aging time required for this study was seven days. The gel formed was rinsed with demineralized water until it was free of ethanol and ammonia. The formed gel was evaporated in an oven at 80 °C and the results are shown in Figure 4.

Figure 4. The synthesis of silica nanoparticles at moles ratio ammonia-ethanol (14:1, 21:1, 28:1, and 42:1)

Characterization of the adsorbent functional groups

The functional groups of the synthesized NS adsorbents (14:1, 21:1, 28:1, and 42:1) were identified using an infrared spectrophotometer in the wavenumber range of 400–4000 cm^{-1} and the results are presented in Figure 5.

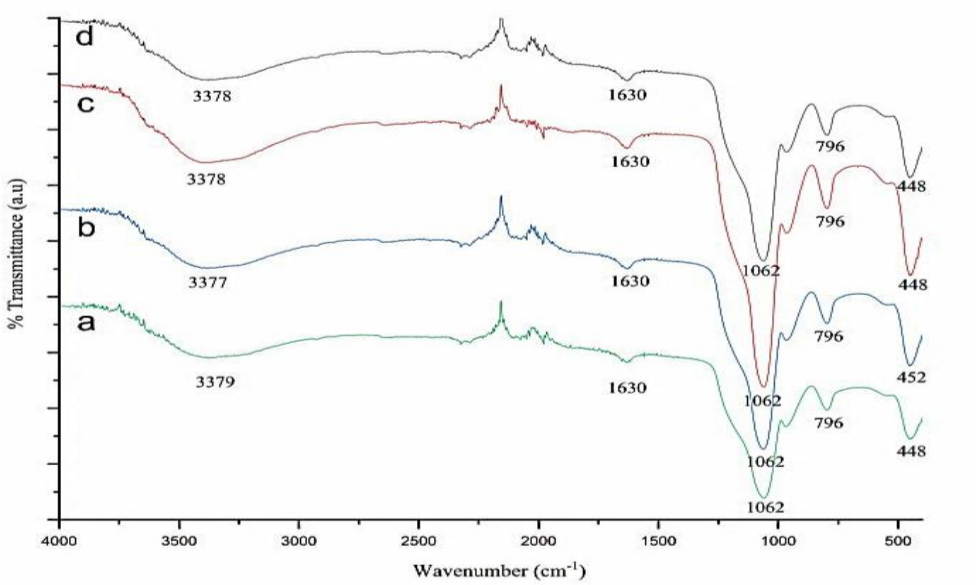

Figure 5. The NS adsorbent spectra results (**a**) 14:1, (**b**) 21:1, (**c**) 28:1, (**d**) 42:1

Figure 5(a) shows that silica nanoparticles have a wavenumber of 3379 cm^{-1}, indicating the presence of OH stretching (Wibowo et al., 2018). The existence of the OH group is also strengthened by the wavenumber at 1630 cm^{-1} show OH bending vibrations (Hayati et al., 2017). The wavenumber proved the Si-O asymmetric stretching at 1062 cm^{-1} (Meliyana et al., 2019), and the peak at 796 cm^{-1} showed Si-O stretching vibration symmetry (Syukri et al., 2017). Si-O bending vibration was observed at 448 cm^{-1} (Al-Abboodi et al., 2020). The FTIR data indicated silica networks and their matched spectra with those of earlier research conducted by Zulfiqar et al. (2016). This research confirmed successful synthesis. A comparison of the silica nanoparticles wavenumbers with those of Kiesel gel 60 from Azmiyawati et al. (2019) is presented in Table 4.

Table 4. Comparison of the silica nanoparticle wavenumbers with Kiesel gel 60

Vibration type	Wavenumber (cm^{-1})					
	NS 14:1	**NS 21:1**	**NS 28:1**	**NS 42:1**	**Kiesel gel 60**	**Zulfiqar et al., (2016)**
OH stretching of Si-OH	3379	3377	3397	3378	3415.7	3426
OH bending of Si-OH	1630	1630	1631	1630	1629.7	1637
Si-O asymmetric stretching of Si-O-Si	1062	1062	1062	1062	1097.4	1094
Si-O symmetric stretching of Si-O-Si	796	796	796	796	800.4	-
Si-O bending of Si-O-Si	448	452	448	448	451.3	466

Size characterization of silica nanoparticles

A Zetasizer nano ZS (Malvern) instrument was employed to evaluate the size of the synthesized silica nanoparticles. The particle size and PdI values for the four variations in silica nanoparticles are listed in Table 5. The particle size of the NS adsorbent is shown in Figure 6.

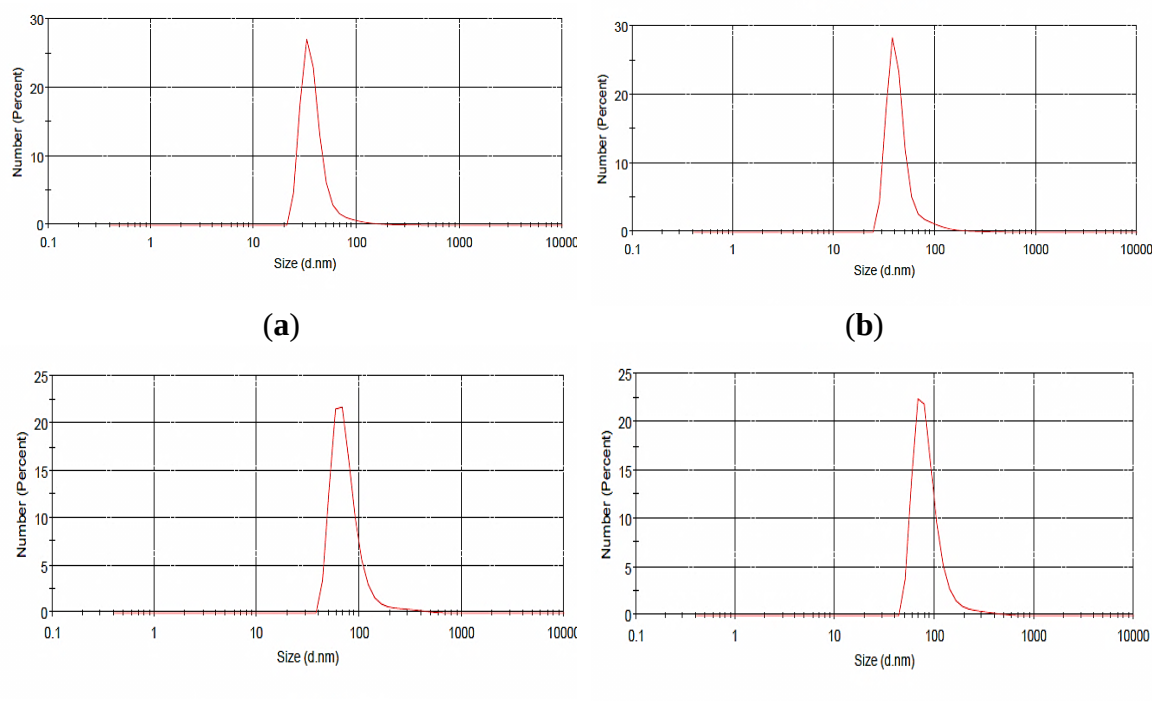

Figure 6. The particle measurement results of NS adsorbent (a) 14:1, (b) 21:1, (c) 28:1, and (d) 42:1

Table 5. The particle size and PdI values of silica nanoparticles

Sample	Particle size (nm)	Polydispersity index (PdI)
NS 14:1	39.82	0.362
NS 21:1	46.50	0.489
NS 28:1	79.19	0.427
NS 42:1	89.32	0.490

Based on Figure 6, the optimal result for silica nanoparticles was obtained at NS 14:1, with a particle size of 39.82 nm and a polydispersity index of 0.362. Measurement results for all adsorbents below 100 nm. The synthesized silica nanoparticles were nano scale because they were in the size range of 1-100 nm (Khan et al., 2017). The particle size decreased as the mole ratio of ammonia in the solution increased. The aggregation of primary particles was reduced at higher pH levels with increased ammonia due to greater electrostatic repulsion, resulting in small-sized silica particles. But on the other side, at a lesser pH, with an increase in ethanol, the electrostatic repulsion decreases, and the primary particles gather quickly to form large particles (Zulfiqar et al., 2016).

The PdI is close to 0, suggesting a homogeneous particle size; if it is less than 0.3, it implies monodispersity, and if it is greater than 0.5, it indicates that the particle is highly heterogeneous. The polydispersity index value in Table 5 does not exceed 0.5, which means that the synthesized silica nanoparticles have a homogeneous particle size distribution so that they tend to be physically stable, which prevents the particles from aggregating with each other. The nanoparticles can be employed as support materials in various applications within the tolerance range at a PdI value of 0.7 (Indrasti et al., 2020).

Chemical stability test of silica nanoparticles

The chemical stability of the silica nanoparticles under acidic to alkaline conditions was evaluated in a solution of pH 4-10. The stability test of the silica nanoparticles adsorbent against acids and bases for 24 h showed that the higher the pH, the lower was the stability of the adsorbent. Silica nanoparticles are resistant to acids, so they are not readily soluble in acidic solutions, which prevents the adsorbent from being easily damaged.

At alkaline pH, the stability of the silica nanoparticles begins to decrease. The stability of the four adsorbents at pH 8-10 decreased, as indicated by the large percentage of dissolved silica nanoparticles. A decrease in the weight of the adsorbent suggested a reduction in its stability. Research conducted by Amaria (2012) reported that the stability of silica gel at pH 10 begins to decrease because silica gel dissolves under alkaline conditions. The stability of the adsorbent against pH is shown in Figure 7.

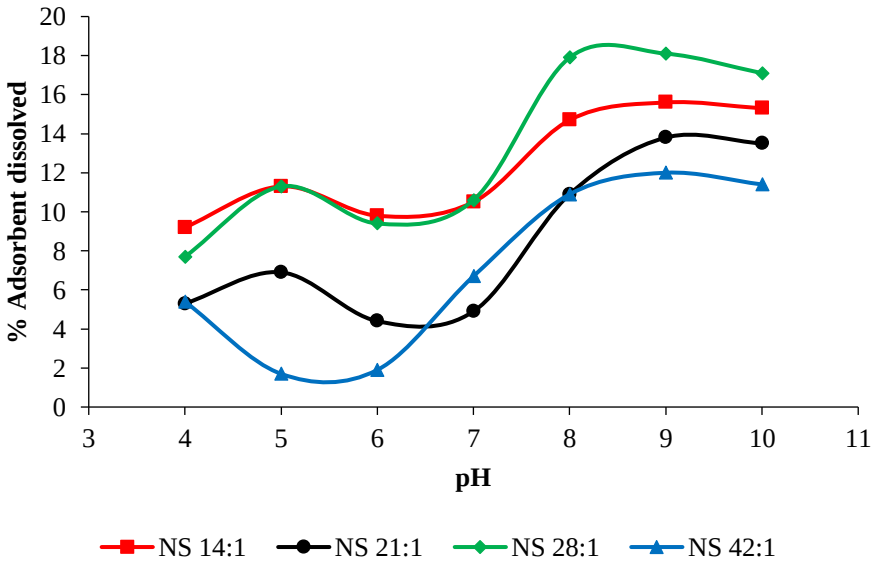

Figure 7. The stability adsorbents against pH

The pH effect on Rhodamine B adsorption

The optimum pH was determined to obtain the best adsorption at various pH values. Rhodamine B is a cationic compound that can form a system under different pH conditions. At pH values below 4, the rhodamine B ions exist as cationic molecules and monomers. Rhodamine B species change from the cationic form to the ionic zwitter form at pH greater than 4 by deprotonation of the carboxyl group (Gan et al., 2013). The structure and species of rhodamine B are shown in Figure 8.

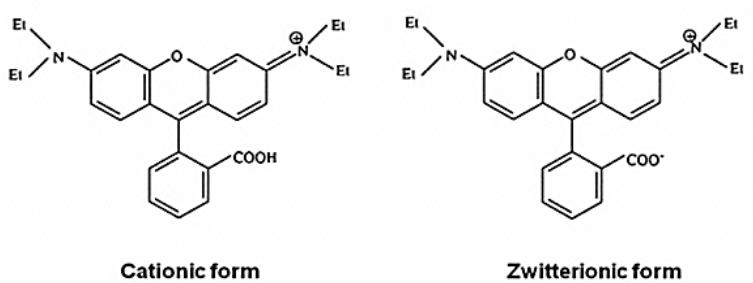

Figure 8. The cationic and zwitterionic structures of rhodamine B

The ionic zwitterform of rhodamine B in water can increase rhodamine B aggregation through the electrostatic reaction between xanthene dye and the carboxyl group (Gan et al., 2013). The adsorbent used at various pH values and contact times was NS 14:1 because it was based on the results of the optimum particle size characteristics and NS 42:1 as a comparison with larger particle sizes. The effect of pH on the adsorption of NS 14:1 and NS 42:1 is shown in Figure 9.

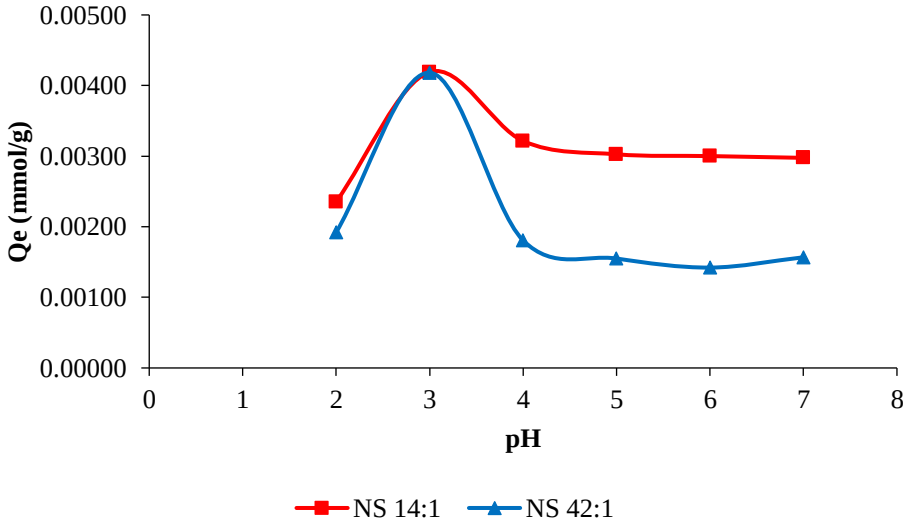

Figure 9. Effect of pH on NS 14:1 and NS 42:1 adsorption

The maximum adsorption by NS 14:1 occurred at a pH 3 of 0.00419 mmol.g^{-1} (44.25%), and NS 42:1 occurred at a pH 3 of 0.00418 mmol.g^{-1} (44.03%). The adsorbent NS 14:1 has a higher adsorption capacity than the adsorbent NS 42:1 because the adsorbent NS 14:1 has smaller particles than the adsorbent NS 42:1, and the smaller particles have larger surface areas, thus increasing the interaction between the adsorbent and adsorbate (rhodamine B).

The contact time effect on Rhodamine B adsorption

The optimum contact time was used to determine the maximum interaction time between the adsorbent and rhodamine B. The study of the effect of adsorption contact time will be used to study adsorption kinetics (Triawan et al., 2017). For the NS 14:1 adsorbent, the optimum adsorption with increasing contact time up to 40 min then tends to be constant after 60 min. Meanwhile, the optimum contact time required by NS 42:1 to adsorption rhodamine B was within 60 min. The contact time tended to be constant after 90 min because the adsorbent surface or the active group reached its saturation point and reached equilibrium. The NS 14:1 adsorbent was able to adsorption an adsorbate was 0.00356 mmol.g^{-1} and the NS 42:1 adsorbent was 0.00279 mmol.g^{-1}. The effect of contact time on the adsorption of NS 14:1 and NS 42:1 is shown in Figure 10.

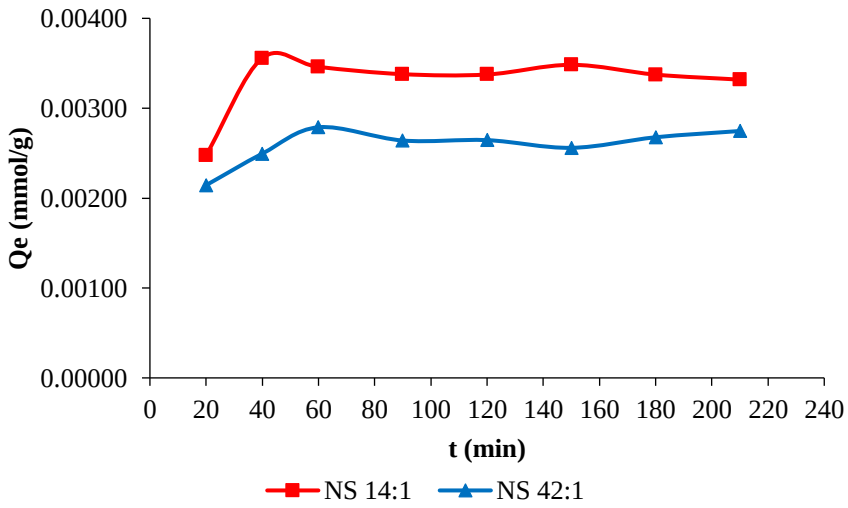

Figure 10. Effect of contact time on NS 14:1 and NS 42:1 adsorption

The adsorption ability of NS 14:1 was higher than that of NS 42:1. Based on the results of the previous characterization, NS 14:1 has an optimum particle size and more uniform particle size distribution than NS 42:1, so that the adsorption ability will be increased by the adsorbent NS 14:1.

The contact time data can be applied to the first-order adsorption kinetics model, which reaches equilibrium and pseudo-second-order to calculate the rate constant for adsorption by each adsorbent. The parameters from some reaction kinetic models for the adsorption of rhodamine B by NS 14:1 and NS 42:1 are presented in Table 6.

Table 6. The reaction kinetics model for adsorption of rhodamine B by NS 14:1 and NS 42:1

Adsorbent	Adsorption kinetics model			
	Pseudo-first order		Pseudo-second order	
	k (min^{-1})	R^2	k ($g.mmol^{-1}.min^{-1}$)	R^2
NS 14:1	0.0759	0.9720	102.42	0.9969
NS 42:1	0.0650	0.8813	162.53	0.9972

Table 6 shows the rate constants for adsorption and coefficients of determination obtained from several kinetic models. The calculation indicates that the pseudo-second-order kinetics adsorption model is suitable because the value of the linear coefficient (R^2) is higher than that of the pseudo-first-order model. Kinetic models show the coefficient of determination (R^2) of pseudo-second order for the NS 14:1 adsorbent of 0.9969 and the NS 42:1 adsorbent of 0.9972. Pseudo-second-order kinetics clearly shows the interrelations between the adsorbent and adsorbate. The rate constants for the adsorption of adsorbents NS 14:1 and NS 42:1 were 102.42 $g.mmol^{-1}.min^{-1}$ and 162.53 $g.mmol^{-1}.min^{-1}$. The NS 14:1 rate constant decreased 1.5 times from the rate constant for the adsorption of NS 42:1. The rate of adsorption of rhodamine B by NS 42:1 was slightly faster than that of NS 14:1.

Conclusions

Silica nanoparticles were successfully synthesized at various ammonia-to-ethanol mole ratios. The FTIR results showed that all adsorbents had functional

groups, indicating the presence of silica. The optimum mole ratio of ammonia to ethanol was 14:1 with a particle size of 39.82 nm. The maximum adsorption of rhodamine B using adsorbent NS 14:1 occurred at a pH 3 of 0.00419 $mmol.g^{-1}$, contact time of 40 min, and rate constant adsorption of 102.42 $g.mmol^{-1}.min^{-1}$ followed a pseudo-second-order kinetic model. In perfecting the research that has been done, further analysis is needed regarding the use of different mole ratios of ethanol to determine the formation of synthesized particles and further characterization to support data from previous characterization results.

References

Aini, N. and Amaria, 2022. Sintesis Nanopartikel Au-SiO_2 Menggunakan Natrium Silikat dari Abu Ampas Tebu (AAT). , 11(3), pp.143–152.

Al-Abboodi, S.M.T., Al-Shaibani, E.J.A. and Alrubai, E.A., 2020. Preparation and Characterization of Nano silica Prepared by Different Precipitation Methods. *IOP Conference Series: Materials Science and Engineering*, 978(1), pp.1–12.

Amaria, 2012. Adsorpsi Ion Sianida dalam Larutan Menggunakan Adsorben Hibrida Aminopropil Silika Gel dari Sekam Padi Terimpregnasi Aluminium. *J. Manusia dan Lingkungan*, 19(1), pp.56–65.

Asnawati, Kharismaningrum, R.R. and Andarini, N., 2017. Penentuan Kapasitas Adsorpsi Selulosa terhadap Rhodamin B dalam Sistem Dinamis. *Jurnal Kimia Riset*, 2(1), pp.23–29.

Azmiyawati, C., Niami, S.S. and Darmawan, A., 2019. Synthesis of silica gel from glass waste for adsorption of Mg^{2+} , Cu^{2+} , and Ag^{+} metal ions. *IOP Conf. Series: Materials Science and Engineering*, 509, pp.1–5.

Beganskiene, A., Sirutkaitis, V., Kurtinaitiene, M., Juskenas, R. and Kareiva, A., 2004. FTIR, TEM and NMR Investigations of Stöber Silica Nanoparticles. *Materials Science*, 10(4), pp.287–290.

Bhatt, N., Mishra, A., Goswami, R. and Prasad, B., 2021. Preparation of Silica Nano-Particles by Sol-Gel Method and Its Characterization. *Journal of Graphic Era University*, 9(2), pp.215–230.

Gan, P.P., Fong, S. and Li, Y., 2013. Efficient removal of Rhodamine B using a rice hull-based silica supported iron catalyst by Fenton-like process. *Chemical Engineering Journal*, 229, pp.351–363.

Hayati, D., Pardoyo and Azmiyawati, C., 2017. Pengaruh Variasi Jenis Asam terhadap Karakter Nanosilika yang Disintesis dari Abu Sekam Padi. *Jurnal Kimia Sains dan Aplikasi*, 20(1), pp.1–4.

Ibrahim, I.A.M., Zikry, A.A.F. and Sharaf, M.A., 2010. Preparation of spherical silica nanoparticles: Stober silica. *Journal of American Science*, 6(11), pp.985–989.

Indrasti, N.S., Ismayana, A., Maddu, A. and Utomo, S.S., 2020. Synthesis of nano-silica from boiler ash in the sugar cane industry using the precipitation method. *International Journal of Technology*, 11(2), pp.422–435.

Indrawati, D. and Cahyaningrum, S.E., 2013. Pengaruh Perbandingan Komposisi Kitosan dan Silika Terhadap Karakterisasi Adsorben Kitosan-Silika Bead. , 2(1), pp.8–13.

Khan, Ibrahim, Saeed, K. and Khan, Idrees, 2017. Nanoparticles: Properties, applications and toxicities. *Arabian Journal of Chemistry*, pp.1–23.

Kurniasih, M., Riapanitra, A. and Rohadi, A., 2014. Adsorpsi Rhodamin B dengan Adsorben Kitosan Serbuk dan Beads Kitosan. *Jurnal Sains dan Matematika*, 2(2).

Madina, F.E., Elvia, R. and Candra, I.N., 2017. Analisis Kapasitas Adsorpsi Silika dari Pasir Pantai Panjang Bengkulu Terhadap ;Pewarna Rhodamin B. *Jurnal Pendidikan dan Ilmu Kimia*, 1(2), pp.98–101.

Meliyana, Rahmawati, C. and Handayani, L., 2019. Sintesis Nano Silika dari Abu Sekam Padi Dengan Metode Sol Gel. *Prosiding Seminar Nasional Multidisiplin Ilmu Universitas Asahan*. 2019 pp. 800–807.

Nopianingsih, N., Sudiarta, I. and Sulihingtyas, W., 2015. Sintesis Silika Gel Terimobilisasi Difenilkarbazon Dari Abu Sekam Padi Melalui Teknik Sol Gel. *Jurnal Kimia*, 9(2), pp.226–234.

Raditya S., B. and Hendiyanto C., O., 2016. Pemanfaatan Kulit Durian Sebagai Adsorben Logam Berat Pb Pada Limbah Cair Elektroplating. *Jurnal Ilmiah Teknik Lingkungan*, 8(1), pp.10–18.

Sahara, E., Gayatri, P.S. and Suarya, P., 2018. Adsorpsi zat warna rhodamin-B dalam larutan oleh arang aktif batang tanaman gumitir teraktivasi asam fosfat. *Cakra Kimia (Indonesian E-Journal of Applied Chemistry*, 6(1), pp.37–45.

Schubert, U. and Husing, N., 2000. *Synthesis of Inorganic Materials*, Wiley-VCH Verlag GmbH, D-69469 Weinheim, Federal Republic of Germany.

Shofiyani, A., Rahmiyati, Y. and Zaharah, T. anita, 2020. Nanosilika Berbahan Dasar Batu Padas Sebagai Adsorben Zat Warna Sintetis Rhodamin B. *Indonesian Journal of Chemical Science*, 9(3), pp.188–193.

Syukri, I., Hindryawati, N. and S, R.R.D. julia N., 2017. Sintesis Silika dari Abu Sekam Padi Termodifikasi 2-Merkaptobenzotiazol untuk Adsorpsi Ion Logam Cd^{2+} dan Cr^{6+}. *Jurnal Atomik*, 2(2), pp.221–226.

Triawan, D.A., Nesbah and Fitriani, D., 2017. Crude Palm Oil's (CPO) Fly Ash as a Low-Cost Adsorben for Removal of Methylen Blue (MB) from Aqueous Solution. *Jurnal Kimia Riset*, 2(1), pp.10–15.

Ulya, A., Nasra, E., Amran, A. and Kurniawati, D., 2022. Adsorpsi Zat Warna Rhodamine B Dengan Karbon Aktif Kulit Durian Sebagai Adsorben. *Periodic*, 11(2), pp.74–77.

Wibowo, E.A.P., Arzanto, A.W., Maulana, K.D. and Rizkita, A.D., 2018. Preparasi dan Karakterisasi Nanosilika dari Jerami Padi. *Jurnal Ilmiah Sains*, 18(2), pp.35–39.

Wulandari, D.A. and Amaria, 2015. Kapasitas Adsorpsi Silika Abu Sekam Padi Termodifikasi Arginin Untuk Adsorpsi Ion Logam Cr(VI). *UNESA Journal of Chemistry*, 4(1), pp.17–24.

Yusmaniar, Purwanto, A., Putri, E.A. and Rosyidah, D., 2017. Adsorption of Pb(II) using silica gel composite from rice husk ash modified 3-aminopropyltriethoxysilane (APTES)-activated carbon from coconut shell. *AIP Conference Proceedings*.

Yusuf, M., Suhendar, D. and Hadisantoso, E.P., 2014. Studi Karakteristik Silika Gel Hasil Sintesis Dari Abu Ampas Tebu Dengan Variasi Konsentrasi Asam Klorida. *UIN SGD Bandung*, VIII(1), pp.16–28.

Zhai, Q.Z., 2020. Study on SBA-15 as an effective sorbent for dye butyl rhodamine B. *Journal of Sol-Gel Science and Technology*, 96(1), pp.34–46.

Zulfiqar, U., Subhani, T. and Husain, S.W., 2016. Synthesis of silica nanoparticles from sodium silicate under alkaline conditions. *Journal of Sol-Gel Science and Technology*, pp.1–6.